Journal of the American College of Cardiology
© 2002 by the American College of Cardiology Foundation
Published by Elsevier Science Inc.

Vol. 40, No. 3, 2002
ISSN 0735-1097/02/$22.00
PII S0735-1097(02)01975-7

Triggers of Ventricular Tachyarrhythmias and Therapeutic Effects of Nicorandil in Canine Models of LQT2 and LQT3 Syndromes

Masaomi Chinushi, MD,* Hidehiro Kasai, MD,† Minoru Tagawa, MD,† Takashi Washizuka, MD,† Yukio Hosaka, MD,† Yuko Chinushi, MD,† Yoshifusa Aizawa, MD†

Niigata, Japan

OBJECTIVES We sought to identify the triggers of ventricular tachyarrhythmia (VTA) in experimental models of long QT type 2 (LQT2) and long QT type 3 (LQT3) syndromes.

BACKGROUND Most adverse cardiac events occurring in the long QT type 1 syndrome are related to sympathetic nerve activity. In contrast, various factors may trigger VTA in patients with LQT2 and LQT3.

METHODS The mode of onset of VTA and therapeutic effects of the potassium-adenosine triphosphate channel opener nicorandil were compared in canine models of LQT2 and LQT3, using three induction protocols: 1) bradycardia produced by atrioventricular block (BRADY); 2) programmed ventricular stimulation; and 3) electrical stimulation of the left stellate ganglion (left stellate stimulation [LSS]). Transmural unipolar electrograms were recorded, and the activation-recovery interval (ARI) was measured.

RESULTS Ventricular tachyarrhythmias developed during BRADY in all six experiments in the LQT3 model, but in none of the six experiments in LQT2. Programmed ventricular stimulation induced VTA in two experiments of the LQT2 model, but in none of the LQT3 experiments. Stimulation of the left stellate ganglion induced VTA in three experiments in LQT2 and in two experiments in LQT3. Nicorandil caused greater shortening of ARI and greater attenuation of transmural ARI dispersion in the LQT2 model than in the LQT3 model. After treatment with nicorandil, a single VTA was induced in the LQT2 model by LSS, whereas in the LQT3 model, VTA remained inducible by BRADY in four experiments and LSS in one experiment.

CONCLUSIONS An abrupt increase in sympathetic activity appeared arrhythmogenic in both models. Nicorandil attenuated the heterogeneity of ventricular repolarization and suppressed the induction of VTA in the LQT2 model, but had a limited therapeutic effect in the LQT3 model. (J Am Coll Cardiol 2002;40:555–62) © 2002 by the American College of Cardiology Foundation

Recent genetic and molecular studies have shown that some inheritable rhythm disturbances may be caused by genetically determined myocardial ion channel abnormalities (1,2). Thus far, particularly detailed analyses have been carried out in congenital long QT syndrome (LQTS), with six subtypes identified in Romano-Ward syndrome and two in Jervell-Nielsen syndrome (3). Because LQTS is classified on the basis of abnormalities in the gene of myocardial ion channels, the mode of onset of ventricular tachyarrhythmia (VTA) and therapeutic effects of some interventions may vary among subtypes of the syndrome (4,5). Most adverse cardiac events occurring in long QT type 1 syndrome (LQT1) are related to sympathetic nerve activity and are effectively prevented by beta-adrenergic blockade (6,7). In contrast, a number of factors may trigger VTA in patients with LQT2 and LQT3 (6).

To determine the modes of onset of VTA in LQT2 and LQT3, the inducibility of VTA by three different induction protocols was compared in canine models of LQT2 and LQT3: 1) bradycardia caused by atrioventricular block (BRADY); 2) programmed ventricular stimulation (PVS); and 3) electrical stimulation of the left stellate ganglion (left stellate stimulation [LSS]). The therapeutic effects of the potassium-adenosine triphosphate (K-ATP) opener nicorandil were also examined.

METHODS

Surgical preparation. The present study was approved by the Animal Studies Subcommittee of our Institutional Review Board. Experiments were performed on twelve 24- to 36-week-old beagles. The dogs were anesthetized with sodium thiopental (17.5 mg/kg intravenous bolus, followed by a maintenance dose of 5.0 mg/kg per h), intubated and ventilated with an animal respirator. Catheters were inserted into the femoral vein for administration of fluids and drugs and into the femoral artery to monitor blood pressure. Electrocardiographic leads I, II and aVF and blood pressure were continuously monitored. The heart was exposed through a midline sternotomy. A core temperature was maintained constant at 37°C with a thermostatically con-

From the *School of Health Science and †First Department of Internal Medicine, Niigata University School of Medicine, Niigata, Japan. This work was supported in part by funds from a grant for research on coronary artery disease from the Japan Heart Foundation Pfizer Pharmaceuticals and by funds provided to Dr. M. Chinushi from the Fukudakinen Iryougijitu Foundation.

Manuscript received December 3, 2001; revised manuscript received March 19, 2002, accepted April 30, 2002.

Abbreviations and Acronyms

ARI	= activation-recovery interval
BCL	= basic cycle length
BRADY	= bradycardia produced by atrioventricular block
K-ATP	= potassium-adenosine triphosphate
LSS	= left stellate (ganglion) stimulation
LQTS	= long QT syndrome
LQT1	= long QT type 1 syndrome
LQT2	= long QT type 2 syndrome
LQT3	= long QT type 3 syndrome
PVS	= programmed ventricular stimulation
VTA	= ventricular tachyarrhythmia

trolled thermal blanket. Saline warmed to 37°C was regularly applied to the heart to moisten and prevent cooling of the epicardial surface. Bradycardia produced by atrioventricular block was accomplished by radiofrequency catheter ablation of the atrioventricular junction, and right ventricular pacing was performed through endocardial bipolar stainless-wire electrodes. Electrical LSS was performed by the delivery of square pulses (duration of 2 ms, output of 5.0 V and frequency of 10 Hz) through a 75-μm polymide-coated silver wire denuded over 2 to 3 mm at its tip and inserted into the surgically exposed ganglion. Upon completion of the experiment, ventricular fibrillation was induced electrically and the heart was excised.

Recording and pacing electrodes. Four plunge-needle electrodes were inserted in the mid left ventricular myocardium, where prominent M-cell–like activity has been found in canine experimental models (8,9). The needle electrodes were made of polymide-coated tungsten wires, 50 μm in diameter, containing a 21-gauge stainless-steel needle. Each needle supported eight unipolar electrodes 1 mm apart. The most proximal electrode was located ~0.5 mm from the epicardial surface, and unipolar electrograms across the left ventricular walls from the epicardial, mid-myocardial and endocardial sites were recorded simultaneously (8,9). The heart was paced from bipolar electrodes inserted in the right ventricular endocardial site. Pacing pulses 2 ms in duration were delivered by a programmable cardiac stimulator at twice the end-diastolic threshold.

Data acquisition. Each electrogram was amplified and filtered at a fixed high-pass setting of 0.05 Hz and adjustable low-pass setting of 500 Hz. Analog data were digitized at a sampling rate of 1,000 Hz (MacLab System, AD Instruments, NSW, Australia). To estimate local refractoriness, the activation-recovery interval (ARI) was calculated from each unipolar electrogram (10). Activation-recovery interval was defined as the interval between the time of the minimal first derivative of the intrinsic deflection of the QRS complex and the maximal first derivative of the T-wave on the unipolar electrogram (10,11).

Drug administration. In six dogs, LQT2 was simulated with dofetilide dissolved in sterile saline administered as a 20 μg/kg intravenous bolus, followed by a maintenance dose of 0.1 μg/kg/min. In six other dogs, LQT3 was simulated with anthopleurin-A dissolved in sterile saline administered as a 5 μg/kg intravenous bolus, followed by a maintenance dose of 0.2 μg/kg/min. Nicorandil was dissolved in sterile saline and administered intravenously at a rate of 0.2 mg/kg/3 min.

Study protocol. INDUCTION OF VTA. In both LQTS models, three protocols were used to study the inducibility of VTA before and after the administration of nicorandil: 1) bradycardia was produced by radiofrequency ablation of the atrioventricular node, followed by a slow ventricular escape rhythm and back-up demand pacing at an escape interval of 1,500 ms continued for 10 min; 2) PVS with two or three extrastimuli was attempted from the right ventricle during pacing at 600-ms and 400-ms basic cycle lengths (BCLs); 3) sympathetic stimulation was performed for 30 s by LSS

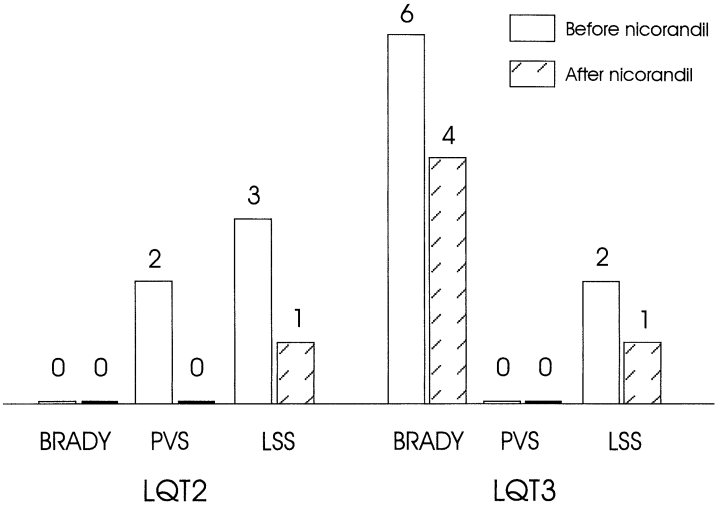

Figure 1. Inducibility of ventricular tachyarrhythmia before and after administration of nicorandil. Each **bar** represents the number of experiments during which ventricular tachyarrhythmias were induced. BRADY = bradycardia produced by atrioventricular block; LQT2 and LQT3 = long QT syndrome, types 2 and 3, respectively; LSS = left stellate (ganglion) stimulation; PVS = programmed ventricular stimulation.

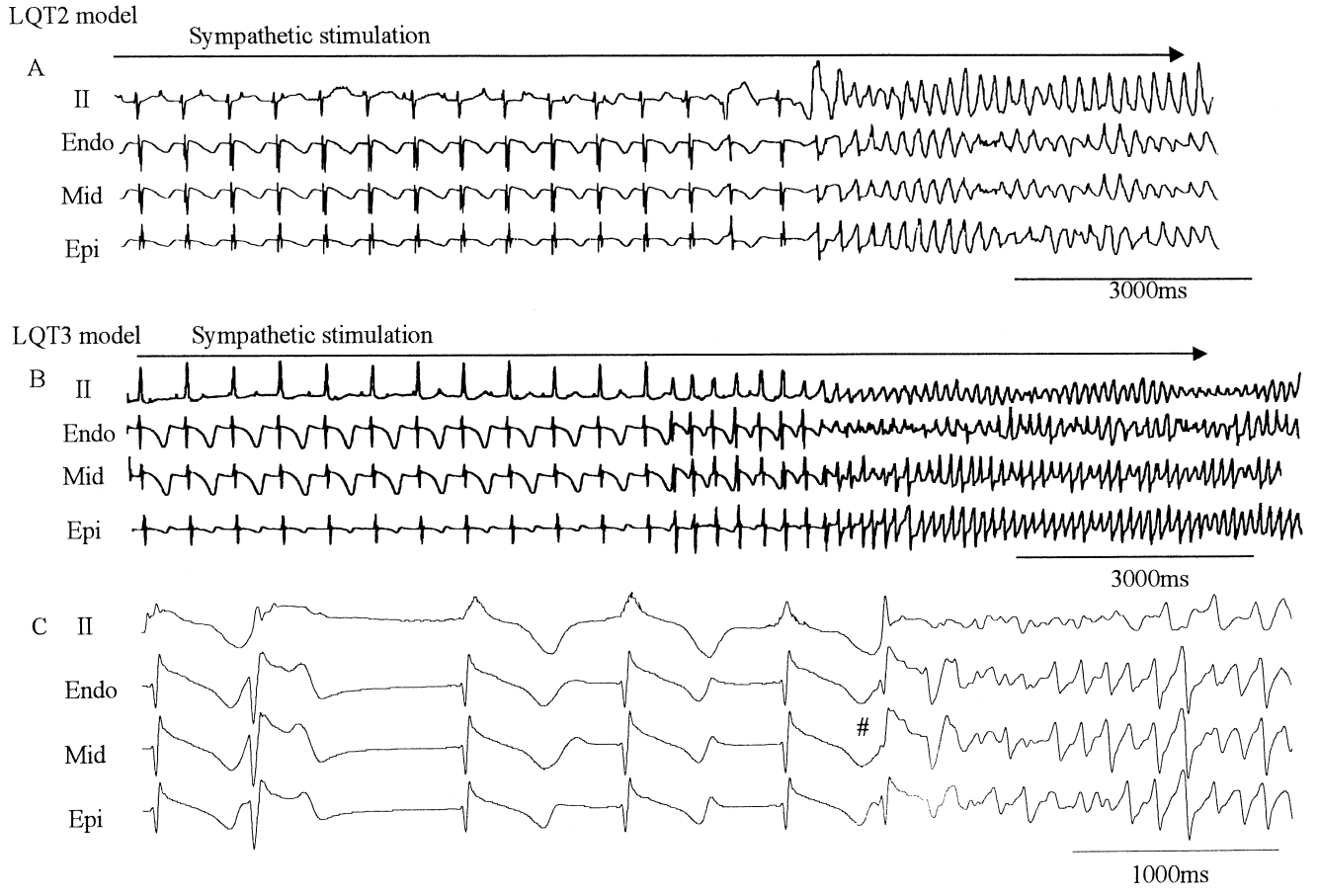

Figure 2. Induction of ventricular tachyarrhythmias (VTAs) in the long QT syndrome type 2 (LQT2) **(A)** and long QT syndrome type 3 (LQT3) **(B and C)** models. During 600-ms basic cycle length pacing, VTA was initiated by a premature beat during left stellate (ganglion) stimulation (LSS) in LQT2 **(A)**. In the LQT3 model, LSS induced multiple premature ventricular complexes and initiated VTA **(B)**. **(C)** Bradycardia produced by atrioventricular block-dependent VTA. A premature ventricular beat **(#)** infringed on spatial dispersion of repolarization and created functional conduction block or delayed conduction at the mid-myocardial site (Mid). Endo = endocardial site; Epi = epicardial site.

during ventricular pacing at 600 ms BCL. When sustained VTA was induced, 5- to 20-J defibrillation shocks were delivered and at least 10 min was allowed to elapse after the shock before continuation of the protocol.

DISTRIBUTION AND TRANSMURAL DISPERSION OF ARI. The ARI at each layer of the ventricle and transmural ARI dispersion were analyzed at 600-ms and 400-ms BCL pacing before administration of nicorandil and at 600-ms BCL pacing after nicorandil. The most proximal and distal plunge electrode sites were used as representatives of the epicardial and endocardial layers, respectively, whereas an intermediate site with the longest ARI at baseline was used a representative of the mid-myocardial site layer. Transmural ARI dispersion was defined as the maximal ARI difference at each needle electrode. An average ARI value was calculated from three consecutive beats at each experimental phase. The beat-to-beat ARI difference was consistently <10 ms during each pacing protocol.

Statistical analysis. Statistical analysis was performed by using the Student *t* test, analysis of variance and Scheffé multiple-range post-hoc test, as appropriate. A p value <0.05 was considered statistically significant. Data are presented as the mean value ± SD.

RESULTS

Induction of VTA and effects of nicorandil. During simulated LQT2 syndrome, VTA did not develop during bradycardia in any of the six experiments (Fig. 1). In contrast, PVS induced VTA in two experiments, and LSS induced VTA in three experiments (Fig. 2A). Administration of nicorandil was followed by a nonstatistically significant decrease in systolic and diastolic blood pressure from 120 ± 14 mm to 109 ± 11 mm Hg and 65 ± 6 mm Hg to 60 ± 8 mm Hg, respectively, during pacing at 600 ms BCL. After the administration of nicorandil, VTA was induced by neither BRADY nor PVS, although it remained inducible by LSS in one experiment. During simulated LQT3 syndrome, spontaneous VTA developed during BRADY in all six experiments (Fig. 2C). In contrast, PVS failed to induce VTA. Stimulation of the left stellate ganglion induced VTA in two experiments. After treatment with nicorandil, spontaneous VTA developed during BRADY in three experi-

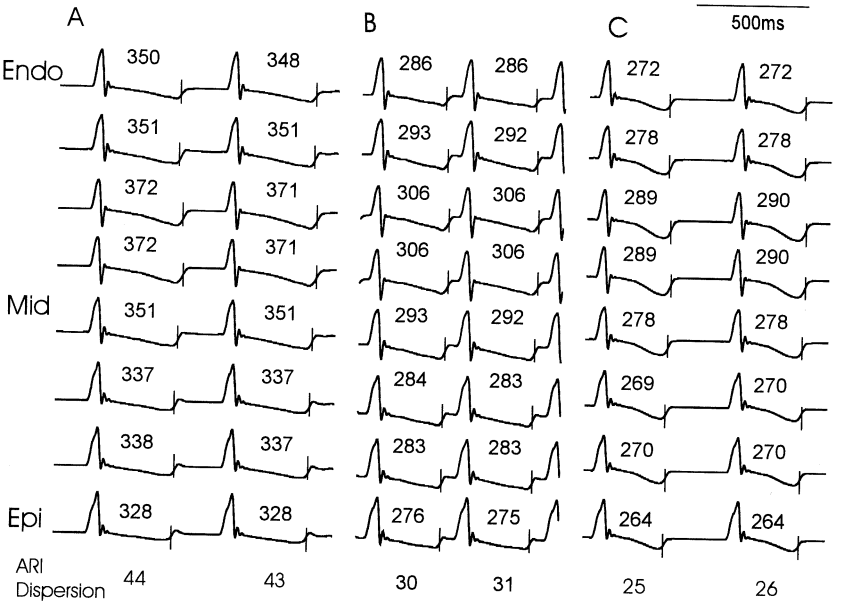

Figure 3. Transmural unipolar recording of the left ventricle in the long QT syndrome type 2 (LQT2) model. The activation-recovery interval (ARI) and its transmural dispersion are presented during pacing at basic cycle lengths (BCLs) of 600 ms **(A)**, 400 ms **(B)** and 600 ms after nicorandil **(C)**. The ARI measurements are shown with each electrogram. The **thin vertical line** in each electrogram represents the point of the maximal derivative of the T-wave. **(A)** The mid-myocardial (Mid) site shows greater ARI prolongation than the epicardial (Epi) or endocardial (Endo) sites, resulting in a 43- to 44-ms ARI dispersion across the ventricular wall. Faster pacing at a 400-ms BCL shortened ARI at all sites, and transmural ARI dispersion was reduced to 30 to 31 ms **(B)**. Compared with faster pacing, the magnitude of ARI shortening was significantly greater when nicorandil was administrated during 600-ms BCL pacing, and transmural ARI dispersion decreased to 25 to 26 ms **(C)**.

ments. In one other experiment, VTA was induced by both LSS and BRADY.

In no experiment did previously noninducible VTA become inducible after the administration of nicorandil.

In both LQTS models, initiation of VTA was associated with the development of conduction block or delayed conduction at the mid-myocardial and endocardial sites, with prolonged ARI at baseline. In all 10 episodes of BRADY-related VTA in the LQT3 model, a short-long-short cardiac sequence or ARI alternans associated with premature ventricular beats (Fig. 2C) was observed before the development of VTA. Among seven episodes of LSS-induced VTA, VTA was initiated after a short-long-short cardiac sequence in five episodes (3 in the LQT2 model and 2 in the LQT3 model) (Fig. 2A), and repetitive premature ventricular beats triggered VTA in two other episodes (one in the LQT2 model and one in the LQT3 model) (Fig. 2B).

The ARI and its transmural dispersion in each model of LQTS. Figure 3 illustrates unipolar recordings from a needle electrode placed in the mid left ventricular myocardium in the LQT2 model. At 600-ms BCL pacing, ARI at the mid-myocardial site was longer than that at the epicardial and endocardial sites, resulting in transmural ARI dispersion of 43 to 44 ms in this area. When the BCL was shortened to 400 ms, the ARIs at all sites were shortened significantly (Table 1), and transmural ARI dispersion decreased to 30 to 31 ms as a result of greater ARI shortening at the mid-myocardial site than at the epicardial site (Table 2). The intravenous administration of nicorandil also shortened the ARIs in all three layers of the ventricle at a drive BCL of 600 ms (Table 1) and decreased ARI dispersion to 25 to 26 ms. The ARIs at 400-ms BCL pacing were statistically longer than those at 600 ms after nicorandil in all three layers of the ventricle (Table 1). In each pacing condition, the ARIs at the mid-myocardial and endocardial sites were statistically longer than those at the epicardial site. Compared with 600-ms BCL pacing before the administration of nicorandil, transmural ARI dispersion was markedly attenuated by both 400-ms BCL pacing and infusion of nicorandil, and transmural ARI dispersion was not significantly different between 400-ms BCL pacing before nicorandil (27.8 $\pm$ 7.7 ms) and 600-ms BCL pacing after nicorandil (22.3 $\pm$ 6.7 ms) (Fig. 4).

Figure 5 shows the same analysis in the LQT3 model and presents unipolar electrograms recorded from a needle electrode in the left ventricle. During 600-ms BCL pacing, ARI at the mid-myocardial site was longer than that at the epicardial and endocardial sites, resulting in marked transmural ARI dispersion of 69 ms. When the pacing BCL was shortened to 400 ms, the ARIs were abbreviated in all three layers of the ventricle (Table 1), but shortening of ARI was considerably greater at the mid-myocardial site than at the epicardial and endocardial sites, and transmural ARI dispersion decreased to 30 to 33 ms. The intravenous administration of nicorandil also shortened ARI, although the effect was weak, resulting in transmural dispersion of 54 to 56 ms. During 600-ms BCL pacing before and after nicorandil administration, ARI at the mid-myocardial site was longer than that at the epicardial site. In contrast, each layer of the ventricle showed similar ARI values during

Table 1. Average Activation–Recovery Interval in Each Condition

	A: 600 ms		B: 400 ms		C: 600 ms+ Nicorandil		p Values	
							A vs. B/A vs. C	B vs. C
LQT2 (n = 24; 6 exp. × 4 needles)								
Endo	355 ± 15		295 ± 7		278 ± 6		<0.0001/<0.0001/<0.0001	
	p = 0.0260		p = NS		p = NS		ANOVA (A,B,C): p<0.0001	
Mid	365 ± 12	p < 0.0001	300 ± 6	p < 0.0001	280 ± 7	p < 0.0001	<0.0001/<0.0001/<0.0001	
	p < 0.0001		p < 0.0001		p < 0.0001		ANOVA (A,B,C): p<0.0001	
Epi	336 ± 9		282 ± 6		269 ± 3		<0.0001/<0.0001/<0.0001	
ANOVA: Endo, Mid and Epi	p < 0.0001		p < 0.0001		p < 0.0001		ANOVA (A,B,C): p<0.0001	
LQT3 (n = 24; 6 exp. × 4 needles)								
Endo	402 ± 20		277 ± 15		367 ± 18		<0.0001/<0.0001/<0.0001	
	p = 0.0041		p = NS		p = 0.0298		ANOVA:A,B,C: p<0.0001	
Mid	422 ± 13	p = 0.0111	280 ± 10	p = NS	381 ± 11	p = NS	<0.0001/<0.0001/<0.0001	
	p < 0.0001		p = NS		p = 0.0014		ANOVA:A,B,C: p<0.0001	
Epi	385 ± 25		273 ± 11		361 ± 24		<0.0001/0.0012/<0.0001	
ANOVA: Endo, Mid and Epi	p < 0.0001		p = NS		p = 0.0010		ANOVA:A,B,C: p<0.0001	
LQT2 vs. LQT3								
Endo vs. Endo	p < 0.0001		p < 0.0001		p < 0.0001			
Mid vs. Mid	p < 0.0001		p < 0.0001		p < 0.0001			
Epi vs. Epi	p < 0.0001		p = 0.0014		p < 0.0001			

Data are presented as the mean value ± SD.
ANOVA = analysis of variance; Endo = endocardium; Epi = epicardium; exp. = experiments; Mid = mid-myocardium.

pacing at 400 ms before the administration of nicorandil (Table 1). In all myocardial layers, ARI was shorter during 400-ms BCL pacing before the administration of nicorandil than at 600 ms after nicorandil administration (Table 1). Before nicorandil, transmural ARI dispersion during 400-ms BCL pacing (21.4 ± 9.0 ms) was significantly less than that at 600 ms (51.2 ± 17.5 ms), although there was no statistically significant difference in transmural ARI dispersion between 600-ms BCL pacing before (51.2 ± 17.5 ms) and after (42.3 ± 12.9 ms) nicorandil infusion (Fig. 4). Finally, transmural ARI dispersion was less during 400-ms BCL pacing before nicorandil administration than during 600-ms BCL pacing after nicorandil administration.

Comparison of ARI and its transmural dispersion between the LQT2 and LQT3 models. During 600-ms BCL pacing before and after nicorandil, the ARIs in the LQT3 model were longer than those in the LQT2 model in all three layers of the ventricle (Table 1). In contrast, the ARIs in all three layers of the ventricle in the LQT2 model became longer than those in the LQT3 model during 400-ms BCL pacing before nicorandil. Transmural ARI dispersion in the LQT3 model was greater than that in the LQT2 model at 600-ms BCL pacing before and after nicorandil, whereas transmural ARI dispersion in the LQT2 model was larger than that in the LQT3 model during 400-ms BCL pacing before administration of nicorandil (Fig. 4). Compared with LQT3, the percentage of ARI shortening by nicorandil was significantly greater in the LQT2 model in all three myocardial layers (Table 2). However, pacing at the shorter BCL of 400 ms was associated with a greater percent shortening of ARI in all myocardial layers in the LQT3 model.

DISCUSSION

Modes of VTA induction. Recent studies have shown that most cardiac events in LQT1 are triggered by sympathetic activity associated with exercise in 62% of patients and emotional stress in 26% (6). In LQT2 syndrome, adverse events have been associated with exercise in 13% of patients, emotional stress in 43% and sleep in 15%; in LQT3, with exercise in 13%, emotional stress in 19% and sleep in 39%. In our canine LQT3 model, the onset of spontaneous VTA was bradycardia-dependent in all six experiments, an observation consistent with previous studies (12,13). Bradycardia produced by atrioventricular block induced marked ARI prolongation at the mid-myocardial site and increased transmural dispersion of repolarization. A short-long-short cardiac sequence and/or ARI alternans associated with premature ventricular beats would facilitate ARI prolongation and enlargement of transmural dispersion of repolarization and could trigger VTA (Fig. 2) (14). In contrast, the onset of VTA was not provoked by BRADY in the LQT2 model (Fig. 1). However, ARI prolongation and transmural ARI dispersion were not as prominent in the LQT2 model than in the LQT3 model during slow heart rates (Fig. 3 and

Table 2. Percent Shortening of the Activation–Recovery Interval by Faster Pacing and Nicorandil Administration

	Endo (%)	Mid (%)	Epi (%)	ANOVA
Faster pacing (BCL 400 ms)		p = 0.135 p < 0.04		
LQT2 (n = 24, 6 exp. × 4 needles)	−16.9 ± 2.7	−17.9 ± 2.8	−16.2 ± 1.0	p < 0.04
		p = 0.268		
		p = 0.043 p < 0.0001		
LQT3 (n = 24, 6 exp. × 4 needles)	−31.2 ± 2.5	−33.5 ± 3.7	−28.8 ± 5.0	p < 0.0004
		p = 0.034		
Comparison between LQT2 and LQT3	p < 0.0001	p < 0.0001	p < 0.0001	
Nicorandil (BCL 600 ms)		p < 0.001 p < 0.0001		
LQT2	−21.8 ± 2.1	−23.3 ± 1.9	−19.8 ± 1.9	p < 0.0001
		p < 0.001		
		p = 0.239 p < 0.0001		
LQT3	−8.8 ± 2.0	−9.6 ± 1.2	−6.1 ± 3.5	p < 0.0001
		p < 0.0004		
Comparison between LQT2 and LQT3	p < 0.0001	p < 0.0001	p < 0.0001	

Data are presented as the mean value ± SD.
ANOVA = analysis of variance; BCL = basic cycle length; other abbreviations as in Table 1.

5). The ARIs in all three layers of the ventricle in the LQT2 model were statistically shorter than those in the LQT3 model during 600-ms BCL pacing (Table 1). Pharmacologic blockade of I_{kr} channels is usually unsuccessful in prolonging the action potential duration to the extent observed in human LQT2 syndrome (13,15,16), and this limitation may have prevented the development of BRADY-dependent VTA in our LQT2 model.

Ventricular tachyarrhythmias were not reliably induced by PVS in the LQT2 or LQT3 model. These results are consistent with the known lack of success of PVS in reproducing VTA during electrophysiologic testing in patients with LQTS, because the first premature stimulus at an intermediate coupling interval or the basic stimulation train, or both, tend to decrease the degree of transmural dispersion of repolarization (9). The total inducibility of

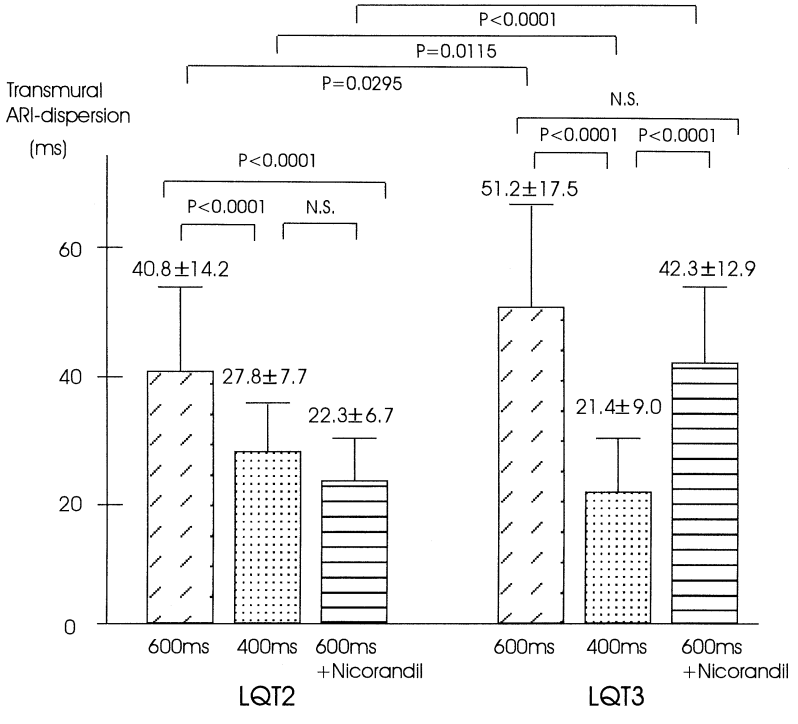

Figure 4. Mean transmural activation-recovery interval (ARI) dispersion in the long QT syndrome type 2 (LQT2) and long QT syndrome type 3 (LQT3) models. See text for details. N.S. = not significant.

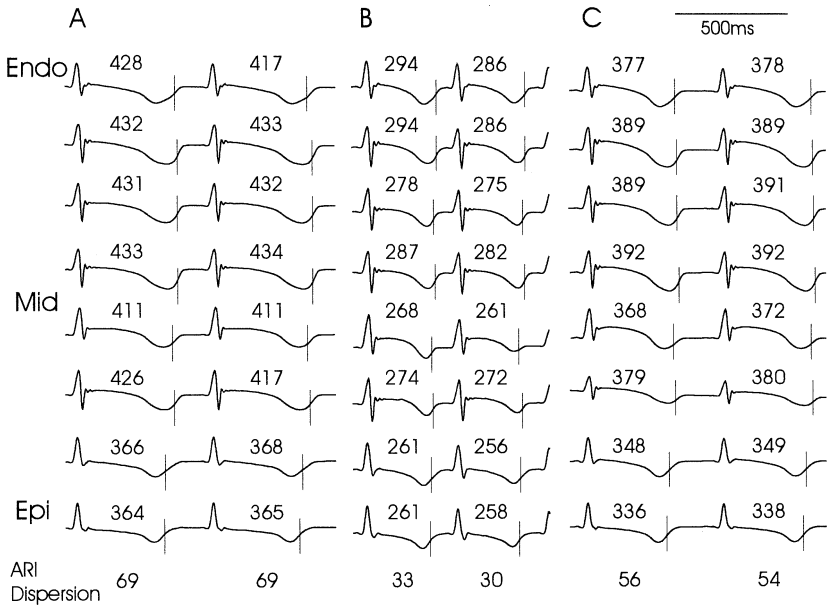

Figure 5. Transmural unipolar recordings of the left ventricle in the long QT syndrome type 3 (LQT3) model, as presented in Figure 3. **(A)** Pacing at 600-ms basic cycle length (BCL). The activation-recovery interval (ARI) at the mid-myocardial (Mid) site was longer than that at the epicardial (Epi) and endocardial (Endo) sites, and marked ARI dispersion of 69 ms was observed across the ventricular wall. Faster pacing at 400-ms BCL **(B)** shortened ARI at all sites, and transmural ARI dispersion was decreased to 30 to 33 ms. Intravenous administration of nicorandil slightly shortened all ARIs at 600-ms BCL pacing **(C)**, and prominent transmural ARI dispersion of 54 to 56 ms persisted across the ventricular wall.

VTA by PVS in the LQT3 model is probably attributable to the adaptive shortening of ARI in response to rapid pacing, which was greater in the LQT3 model than in the LQT2 model (Figs. 3 and 5, Table 2) (15,16).

It is noteworthy that sympathetic stimulation triggered VTA in three simulated LQT2 and two simulated LQT3 experiments. These results are consistent with the precipitation of adverse cardiac events by exercise or emotional stress in both LQT2 and LQT3 syndromes (6). In contrast, sustained beta-adrenergic stimulation has been found to decrease transmural dispersion of repolarization and to suppress VTA in LQT2 and LQT3 experimental models (15,16). Despite this apparently protective effect, the multiple premature beats observed immediately after the onset of LSS may occur at a time when prominent spatial dispersion of repolarization is still present. The results of these LSS experiments suggest that an abrupt increase in sympathetic activity and associated premature beats were arrhythmogenic in both models. Furthermore, in addition to a short-long-short cardiac sequence, repetitive premature ventricular beats triggered VTA in two episodes of LSS-associated VTA (Fig. 2B). The initiation pattern of LSS-induced VTA may be different between the LQT2 and LQT3 models, but this could not be clarified because of the small number of experiments and VTA episodes in the present study.

Antiarrhythmic effect of nicorandil. The therapeutic effects of nicorandil in patients with LQT1 have recently been reported (17). In addition, nicorandil was more effective in the LQT1 and LQT2 models than in the LQT3 model (18). The results of this study are consistent with these clinical and experimental studies—in particular, the greater abbreviation of ARI and larger reduction of transmural ARI dispersion by nicorandil in the LQT2 model than in the LQT3 model. The precise mechanisms of the different response to nicorandil in the two LQTS models have not been clarified. A reduced I_{kr} during phase 3 of the action potential may increase myocardial membrane resistance, and additional currents through K-ATP channels may easily modulate the membrane potential (18). Conversely, an increase in late sodium current can be associated with a smaller membrane resistance in the LQT3 model, and a further net increase in the outward current through the K-ATP channels may have a small effect on the plateau of the action potential. The same hypothesis may be advanced to explain the greater ARI shortening at the mid-myocardial site as compared with the epicardial and endocardial sites (Table 2). The M-cell–like myocardium is characterized by reduced I_{ks} currents, whereas the late sodium current and sodium-calcium exchange current are believed to be increased (19).

Clinical implications. As in LQT1 syndrome, an abrupt increase in sympathetic nerve activity appears arrhythmogenic in LQT2 and LQT3, which may explain the therapeutic effects of beta-blockade in all three subtypes (7). In our experiments, the effect of nicorandil in the LQT2 and LQT3 models was different, although it was antiarrhythmic in both models. Therefore, nicorandil may represent another therapeutic option in LQTS.

Study limitations. Sympathetic nerve stimulation was limited to LSS, and the output was fixed at 5 V. This choice was based on the apparent exaggerated and unbalanced

left-sided sympathetic activity associated with arrhythmogenesis in patients with LQTS (20). Further studies including stimulation of the right stellate ganglion are required to further our understanding of sympathetic activity as an arrhythmogenic factor in LQTS.

The needle electrodes were inserted into the mid left ventricular myocardium, which, in this canine model, exhibited prominent M-cell–like behavior. However, the distribution of M-cell–like activity is heterogeneous (9), such that the limited number of recording electrodes may have underestimated the heterogeneity of ventricular repolarization.

The effects of nicorandil were studied after a single dose. Different doses of nicorandil may have different effects on VTA inducibility and transmural ARI dispersion in these experimental models. Several mutations have been reported in the *HERG* and *SCN5A* genes, and the clinical characteristics of LQTS vary depending on each mutation (21,22). Therefore, experimental studies of drug efficacy using these models are limited in their ability to test the clinical usefulness of therapeutic interventions.

Nicorandil reduced the duration and transmural dispersion of ARI, and its effects were more prominent in the LQT2 model than in the LQT3 model. However, nicorandil produced conflicting results on the induction of VTA, and convincing evidence on nicorandil's protective effect on the inducibility of VTA in the LQT2 versus LQT3 model was not provided because of the small number of experiments in the present study. Further studies with a larger study group are required for detailed analysis of different initiation modes of VTA and the therapeutic effect of nicorandil in the LQT2 and LQT3 models.

Reprint requests and correspondence: Dr. Masaomi Chinushi, School of Health Science, Niigata University School of Medicine, 2-746 Asahimachi Niigata 951-8518, Japan. E-mail: masaomi@clg.niigata-u.ac.jp.

REFERENCES

1. Chen Q, Zhang KG, Brugada R, et al. Genetic basis and molecular mechanism for idiopathic ventricular fibrillation. Nature 1998;392:293–6.
2. Priori SG, Barhanin J, Hauer RN, et al. Genetic and molecular basis of cardiac arrhythmias: impact on clinical management, parts 1 and II. Circulation 1999;99:518–28.
3. Zareba W, Moss AJ, Schwartz PJ, et al., the International Long QT Syndrome Registry Research Group. Influence of genotype on the clinical course of the long QT syndrome. N Engl J Med 1998;339:960–5.
4. Schwartz PJ, Priori SG, Locati EH, et al. Long QT syndrome patients with mutations of the *SCN5A* and *HERG* genes have differential responses to Na channel blockade and to increase in heart rate: implications for gene-specific therapy. Circulation 1995;92:3381–6.
5. Compton SJ, Lux RL, Ramsey MR, et al. Genetically defined therapy of inherited long QT syndrome: correction of abnormal repolarization by potassium. Circulation 1996;94:1018–22.
6. Schwartz PJ, Priori SG, Spazzolini C, et al. Genotype-phenotype correlation in the long QT syndrome: gene-specific triggers for life-threatening arrhythmias. Circulation 2001;103:89–95.
7. Moss AJ, Zareba W, Hall WJ, et al. Effectiveness and limitations of beta-blocker therapy in congenital long-QT syndrome. Circulation 2000;101:616–23.
8. El-Sherif N, Chinushi M, Caref EB, Restivo M. Electrophysiological mechanism of the characteristic electrocardiographic morphology of torsade de pointes tachyarrhythmias in the long QT syndrome. Circulation 1997;96:4392–9.
9. Chinushi M, Caref EB, Restivo M, Noll G, Aizawa Y, El-Sherif N. Cycle length associated modulation of the regional dispersion of ventricular repolarization in a canine model of long QT syndrome. Pacing Clin Electrophysiol 2001;24:1247–57.
10. Haws CW, Lux RL. Correlation between in vivo transmembrane action potential durations and activation recovery intervals from electrograms: effect of interventions that alter repolarization time. Circulation 1991;81:281–8.
11. Chinushi M, Tagawa M, Kasai H, et al. Correlation between effective refractory period and activation-recovery interval calculated from the intracardiac unipolar electrogram of humans in the control and during treatment with *dl*-sotalol. Jpn Circ J 2001;65:702–6.
12. El-Sherif N, Caref EB, Yin H, Restivo M. The electrophysiological mechanism of ventricular tachyarrhythmias in the long QT syndrome: tridimensional mapping of activation and recovery patterns. Circ Res 1996;79:474–92.
13. Shimizu W, Antzelevitch C. Sodium channel block with mexiletine is effective in reducing dispersion of repolarization and preventing torsade de pointes in LQT2 and LQT3 models of the long QT syndrome. Circulation 1997;96:2038–47.
14. Chinushi M, Restivo M, Caref EB, El-Sherif N. The electrophysiological basis of arrhythmogenecity of QT/T alternans in long QT syndrome: tridimentional analysis of the kinetics of cardiac repolarization. Circ Res 1998;83:614–28.
15. Priori SG, Napolitano C, Cantu F, Brown AM, Schwartz PJ. Differential response to Na channel blockade, beta-adrenergic stimulation, and rapid pacing in a cellular model mimicking the *SCN5A* and *HERG* defects present in the long-QT syndrome. Circ Res 1996;78:1009–15.
16. Shimizu W, Antzelevitch C. Differential effects of beta-adrenergic agonists and antagonists in LQT1, LQT2 and LQT3 models of the long QT syndrome. J Am Coll Cardiol 2000;35:778–86.
17. Shimizu W, Kurita T, Matuo K, et al. Improvement of repolarization abnormalities by a K channel opener in the LQT1 form of congenital long QT syndrome. Circulation 1998;97:1581–8.
18. Shimizu W, Antzelevitch C. Effects of a K channel opener to reduce transmural dispersion of repolarization and prevent torsade de pointes in LQT1, LQT2 and LQT3 models of the long QT syndrome. Circulation 2000;102:706–12.
19. Liu DW, Antzelevitch C. Characteristics of the delayed rectifier current (I_{kr} and I_{ks}) in canine ventricular epicardial, mid-myocardial, and endocardial myocytes: a weaker I_{ks} contributes to the longer action potential of the M cell. Circ Res 1995;76:351–65.
20. Zipes DP. The long QT syndrome: a Rosetta stone for sympathetic related ventricular tachyarrhythmias. Circulation 1991;84:1414–9.
21. Yamashita F, Horie M, Kubota T, et al. Characterization and subcellular localization of *KCNQ1* with a heterozygous mutation in the C terminus. J Mol Cell Cardiol 2001;33:197–207.
22. Satler CA, Vessely MR, Duggal P, Ginsburg GS, Beggs AH. Multiple different missense mutations in the pore region of *HERG* in patients with long QT syndrome. Hum Genet 1998;102:265–72.